Polymer Chemistry

Accepted Manuscript

This is an *Accepted Manuscript*, which has been through the Royal Society of Chemistry peer review process and has been accepted for publication.

Accepted Manuscripts are published online shortly after acceptance, before technical editing, formatting and proof reading. Using this free service, authors can make their results available to the community, in citable form, before we publish the edited article. We will replace this *Accepted Manuscript* with the edited and formatted *Advance Article* as soon as it is available.

You can find more information about *Accepted Manuscripts* in the Information for Authors.

Please note that technical editing may introduce minor changes to the text and/or graphics, which may alter content. The journal's standard Terms & Conditions and the Ethical guidelines still apply. In no event shall the Royal Society of Chemistry be held responsible for any errors or omissions in this *Accepted Manuscript* or any consequences arising from the use of any information it contains.

ROYAL SOCIETY OF CHEMISTRY

www.rsc.org/polymers

Cite this: DOI: 10.1039/c0xx00000x

www.rsc.org/xxxxxx

ARTICLE TYPE

Direct Arylation Polycondensation for Efficient Synthesis of Narrow-Bandgap Alternating D-A Copolymers Consisting of Naphthalene Diimide as Acceptor

Jinjun Shao, Guojie Wang, Kai Wang, Cangjie Yang, Mingfeng Wang*

Received (in XXX, XXX) Xth XXXXXXXXX 20XX, Accepted Xth XXXXXXXXX 20XX
DOI: 10.1039/b000000x

A series of narrow-bandgap polymers based on an alkyl-thiophene-flanked naphthalene diimide (TNDI) were synthesized through direct arylation polycondensation. The ^{1}H NMR spectra indicate all polymers correspond to an alternating copolymer structure with good regioregularity. Their photophysical, electrochemical, thermal and charge transport properties are characterized. Among all of the synthesized polymers, the copolymer consisting of alternating TNDI and 4,6-di-(2-thienyl)thieno[3,4-*c*][1,2,5]thiadiazole performs the best in the thin film transistors, with a moderate hole mobility of 4.6 × 10^{-3} cm^2 V^{-1} s^{-1} under ambient condition.

Introduction

Low-bandgap π-conjugated polymers based on the donor-acceptor (D-A) alternating structure are of great importance and interest due to their unique optoelectronic properties and their potential applications such as organic light-emitting diodes (OLEDs),[1] organic thin-film transistors (OTFTs),[2] and organic photovoltaics (OPVs).[3] These π-conjugated polymers are usually synthesized by transition metal-catalyzed cross-coupling techniques such as Suzuki–Miyaura and Migita–Kosugi–Stille couplings.[4] However, these conventional synthetic techniques show disadvantages such as the necessity of prefunctionalization of monomers (arylene diboronic acids and distannyl arylenes) using flammable butyllithium, and particularly for Stille coupling, the difficulty of purifying organotin monomers and the formation of toxic trialkyltin byproducts. To synthesize π-conjugated polymers through an economy-efficient and environment-benign approach, carbon–hydrogen (C–H) direct arylation polycondensation (DAP) reaction has attracted increasing attention recently.[5]

Naphthalene diimide (NDI), due to its excellent electron-transporting properties, has been widely employed to construct high-performance π-conjugated polymers.[6] In addition to serving as n-channel and ambipolar OTFTs, NDI-based polymers have also been employed as electron acceptors to replace fullerene derivatives (PCBMs) in OPVs.[7] Such π-conjugated polymers have been mainly synthesized by Suzuki–Miyaura or Migita–Kosugi–Stille cross-coupling reactions.[6-7] Owing to the promising potential of NDI-based polymers as practical optoelectronic materials, efficient direct arylation polycondensation (DAP) of NDI-based monomers is highly desirable. However, early effort reported by Horie and coworkers[8] using dibrominated NDI as the monomer did not yield high-molecular-weight polymers via DAP, while other dibrominated monomers afforded the corresponding polymers. The inefficient DAP with NDI is presumably a result of interaction of the carbonyl group with a Pd (II) oxidative addition intermediate, which prevents a subsequent C-H bond cleavage. Recently, Nakabayashi and Mori[9] reported that the introduction of alkyl thiophene spacers to NDI by the Migita–Kosugi–Stille coupling provided an improved result in DAP. These results suggest that high-molecular-weight NDI-based polymers can be synthesized by DAP following the appropriate strategy. A microwave-assisted DAP between furan- or thiophene-flanked NDI and 2,3,5,6-tetrafluorobenzene was reported by Sommer et. al.[10] The resulting copolymers with M_n of 7-8 kDa showed electron mobility as high as 1.3 cm^2 V^{-1} s^{-1} in top-gate, bottom-contact OTFT devices.

In this article, we report the synthesis of a series of low-bandgap conjugated polymers (**P1-3**) based on alkyl-thiophene-flanked NDI (**5**) with 3,4-ethylenedioxythiophene (**EDOT**, **8**), 1,4-diketo-3,6-di(thiophen-2-yl)pyrrolo[3,4-c]pyrrole (**DPP**, **9**), and 4,6-di-(2-thienyl)thieno[3,4-*c*][1,2,5]thiadiazole (**TTD**, **7**) (Figure 1) via DAP technique; and their photophysical properties, electrochemical properties, thermal properties and charge transport properties of these polymers are also reported.

Results and discussion

This section starts from the rational molecular design and synthesis of the monomers and the following direct arylation polycondensation towards the three defect-free alternating D-A copolymers shown in Scheme 1. Despite the fact that a variety of NDI-based D-A copolymers has been synthesized via either traditional coupling methods[11] or recently emerging DAP [9,10,12], the chemical structures of the three copolymers (**P1-3**, Scheme 1) are relatively new, and have not been reported so far, to the best of our knowledge. Therefore, we carried out a complete characterization for **P1-3** using ^{1}H-NMR, UV-VIS-NIR absorption spectroscopy, TGA/DSC and cyclovotometry. We further examined the charge carrier mobility of our polymers in field effect transistor (FET) devices and studied how the chemical structure and film morphology affect the device performance.

Synthesis and structural characterization

To enhance the reactivity of NDI derivatives as monomers in direct arylation polycondensation,[8-9] we started from the synthesis of an alkylthiophene-flanked NDI derivative, Compound **4** (Scheme 1). The synthetic routes to Monomers **5**, **7** and Polymers **P1-3** are shown in Scheme 1. Compound **2** was achieved by reacting **1** with flexible amine in refluxing acetic acid for 30 min with a yield of 25%,[13] which was later subjected to Stille coupling reaction with **3**, resulting in 3-ethylhexyl-thiophene-flanked NDI (**4**) with a yield of 93%. Compound **4** was brominated to get Monomer **5** by using NBS as the bromination agent in a mixture of DMF/$CHCl_3$ with 95% yield. Our initial effort of reducing 3',4'-dinitro-2,2':5',2''-terthiophene (**6**) with hydrazine in presence of catalytic Pd/C[14] failed to give the target di-amine intermediate. Nevertheless, the reduction of **6** via tin (II) chloride dihydrate resulted in the di-amine intermediate, which was subsequently reacted with PhNSO/TMSCl in $Et_3N/CHCl_3$ to afford the monomer **TTD 7** with 76% yield in two steps.[15]

Since the presence of backbone defects in the polymer chain can significantly compromise the electronic structures and their thin film properties, well-defined molecular structures with minimal structural defects are indeed favourable during the synthesis of π-conjugated polymers.[16] Our initial attempt of polymerization (data not shown), under the optimized synthetic protocol of DAP that we reported previously,[17] between EDOT and a monomer similar to Compound **5** but without the ethyl-hexyl groups on the thiophene units resulted in some homocoupling byproducts that could be detected by GPC. As a result, using the alkyl

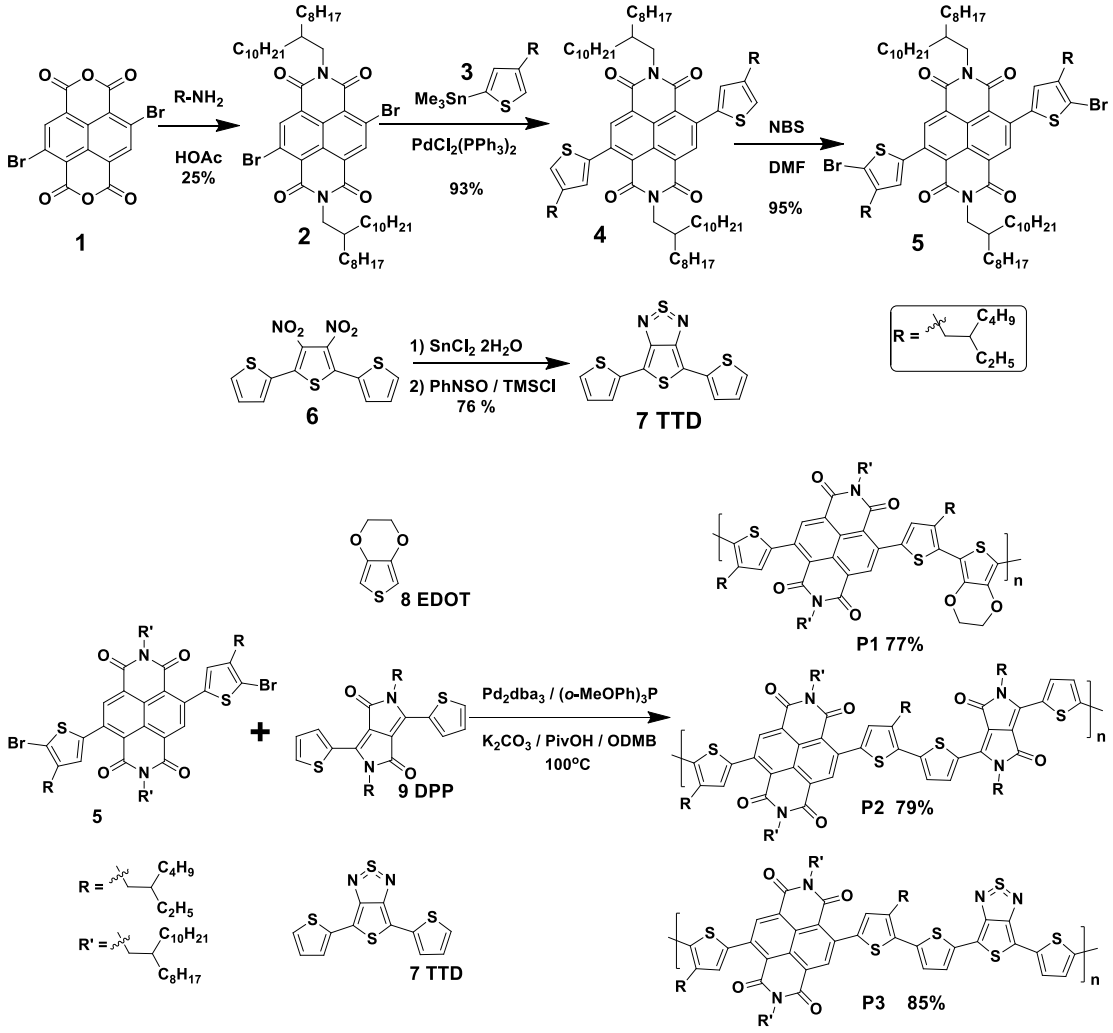

Scheme 1. Synthetic route to polymers **P1**, **P2** and **P3**.

substituents at the *β*-position of thiophene moiety in the monomer **5**, we expected to avoid the side reactions (*β*-defects)[5e] at the β-position of thiophene during DAP reaction. The brominated monomer **5** was used to prepare the copolymers by reacting with the non-activated thiophene derivatives **8**, **9** and **7** via direct DAP to give Polymers **P1-3**, respectively. More synthetic details are described in Experimental Section. After purification by reprecipitation and consecutive Soxhlet extractions, **P1-3** were obtained with a good yield of 77%, 79% and 85%, respectively.

The ^{1}H NMR spectra of **P1-3** were measured in $C_2D_2Cl_4$ at

373 K. The clear spectra confirmed that all of the polymers correspond to an alternating copolymer (Figure 1). The peaks at 8.86 (peak ***a***) and 7.28 ppm (peak ***b***) for all the polymers **P1**, **P2** and **P3** correspond to the protons from naphthalene diimide (NDI) moiety and ethylhexyl thiophene unit, respectively. For **P3**, although the 7.28 ppm peak was overlapped with the peaks from the thiophene unit in the **TTD** (**7**) moiety, the sharp singlet peak could be observed apparently. All the peaks in the ^{1}H NMR spectra can be clearly assigned to each of the polymers (**P1-3**). The small residual peaks (1-3) in the ^{1}H NMR spectra (with a relative integration of about 1-2%) can be assigned to the terminal ending monomer units.[18] The results above indicate that all of the polymers (**P1-3)** possess a well-defined alternating copolymer structure and minimal structural defects, which could benefit the device application.

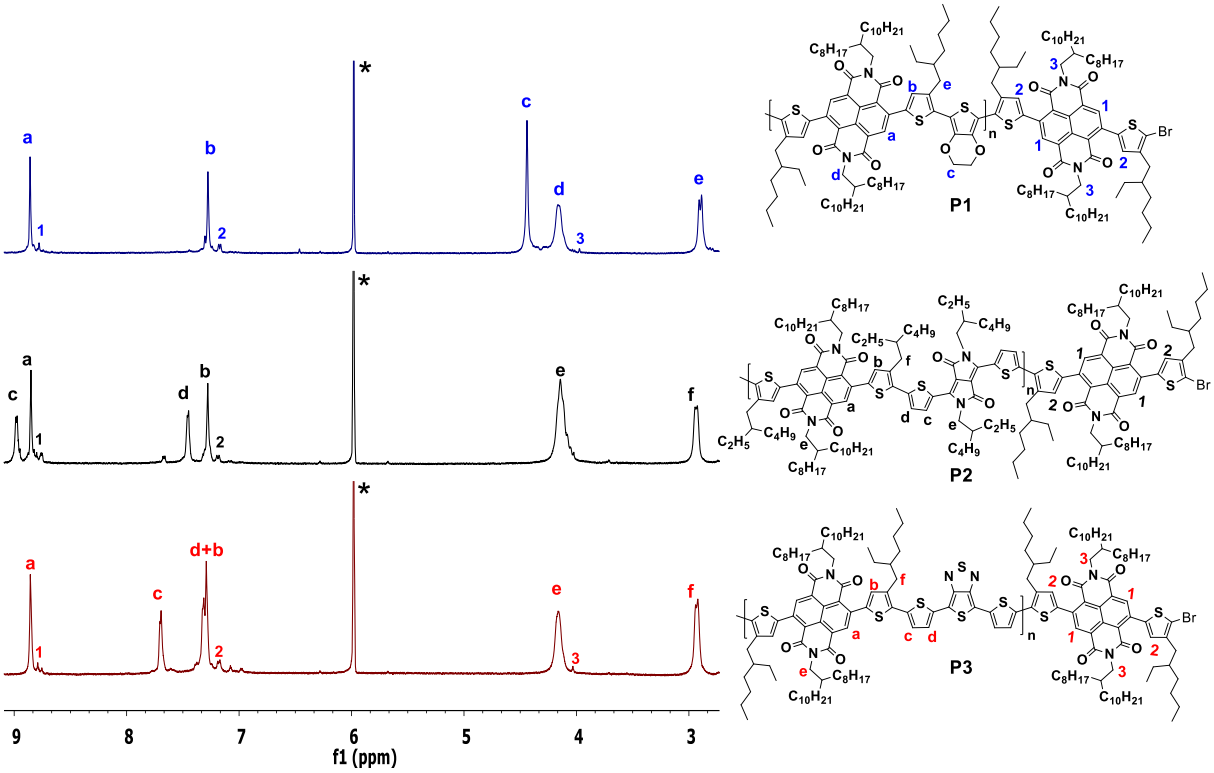

Figure 1. ^{1}H NMR spectra of polymers **P1**, **P2** and **P3** in $C_2D_2Cl_4$ at 373 K.

Table 1. Molecular weights (GPC) data and reaction yields for the Polymers **P1**, **P2** and **P3.**

Polymer	M_n [a] (kDa)	M_w [b] (kDa)	PDI [c]	Yield [d]
P1	16.4	33.3	2.0	77%
P2	27.4	50.5	3.0	79%
P3	17.0	55.4	3.2	85%

[a] Number-average molecular weight (M_n); [b] Weight-average molecular weight (M_w); [c] Polydispersity index (M_w/M_n) determined by means of GPC with THF as eluent on the basis of polystyrene calibration.

These new polymers have good solubility in common organic solvents such as THF, $CHCl_3$ and DCM. Their molecular weight (M_n) and polydispersity index (PDI) were measured by gel permeation chromatography (GPC) using THF as the solvent and polystyrene as the standard. The M_n (PDI) values are 16.4 kDa (2.0), 27.4 kDa (3.0) and 17.0 kDa (3.2) for **P1**, **P2** and **P3**, respectively.

Photophysical properties

The UV-VIS-NIR absorption spectra of **P1**, **P2** and **P3** were recorded in both chloroform solution and drop-coat thin films. The spectra are shown in Fig. 2 and the relevant data are summarized in Table 2. Broad absorption bands across the visible and near infrared (NIR) region were observed for both solution and thin films of **P1**, **P2** and **P3** (Fig. 1). The absorption maxima for **P1**, **P2** and **P3** in solutions are located at 680, 605 and 770 nm, respectively. In the thin films, the absorption spectra showed the absorption maxima at 752, 720 and 835 nm, with obvious red shifts of 72, 115 and 65 nm for **P1**, **P2** and **P3**, respectively, indicating favourable aggregation in the solid thin films. In addition, the occurrence of strong intermolecular interactions which provoke the polymer backbone rigidity is evident in the UV-vis spectra profiles as well. The corresponding optical energy gaps E_g^{opt} estimated from the lowest-energy absorption edge of the absorption spectra in film were calculated to be 1.14, 1.15 and 0.93 eV for **P1**, **P2** and **P3**, respectively, (Table 2).

Electrochemical properties

The electrochemical properties of **P1**, **P2** and **P3** were investigated by cyclic voltammetry (CV) in DCM solution. As

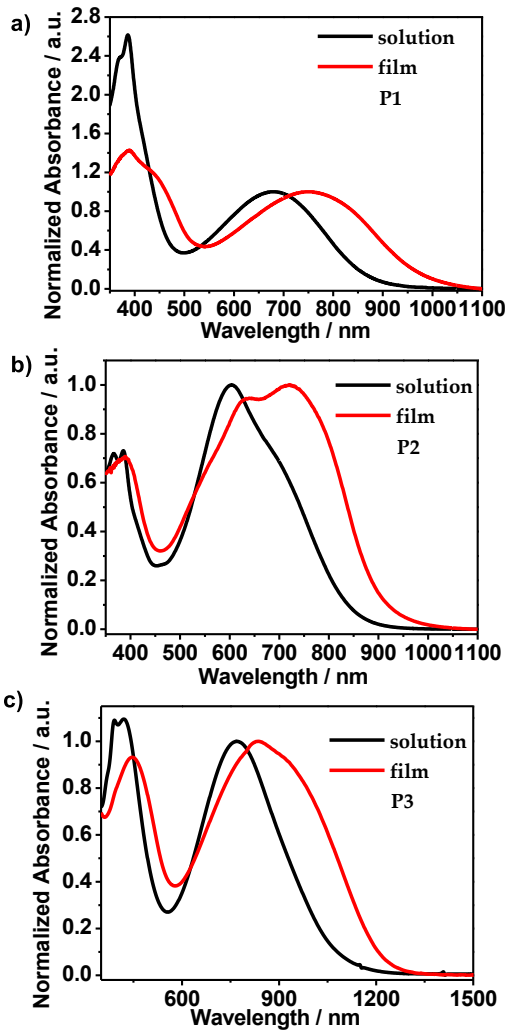

Figure 2. UV-vis absorption spectra of polymers **P1**, **P2** and **P3** in $CHCl_3$ solution and drop-cast films.

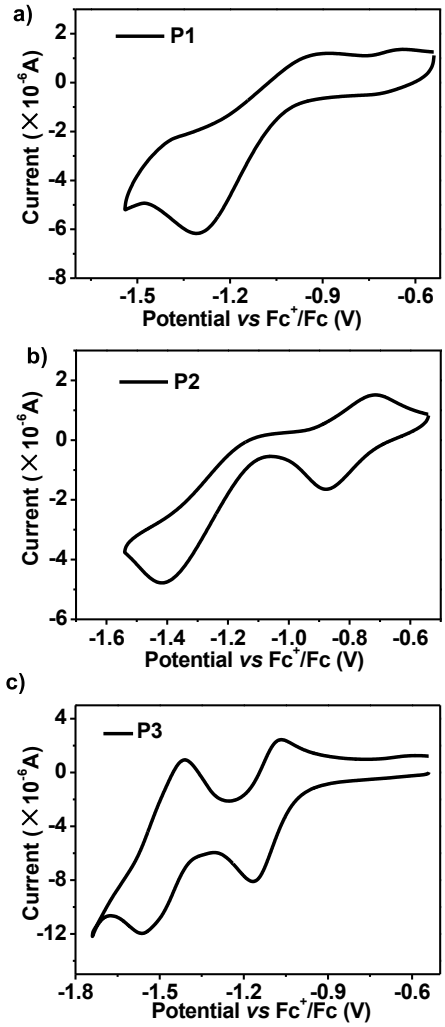

Figure 3. Cyclic voltammograms in dry DCM with 0.1 M Bu_4NPF_6 as supporting electrolyte, a Pt electrode with a diameter of 2 mm, a Pt wire, and an Ag/AgCl electrode were used as the working electrode, the counter electrode, and the reference electrode, respectively, with a scan rate at 50 mV/s.

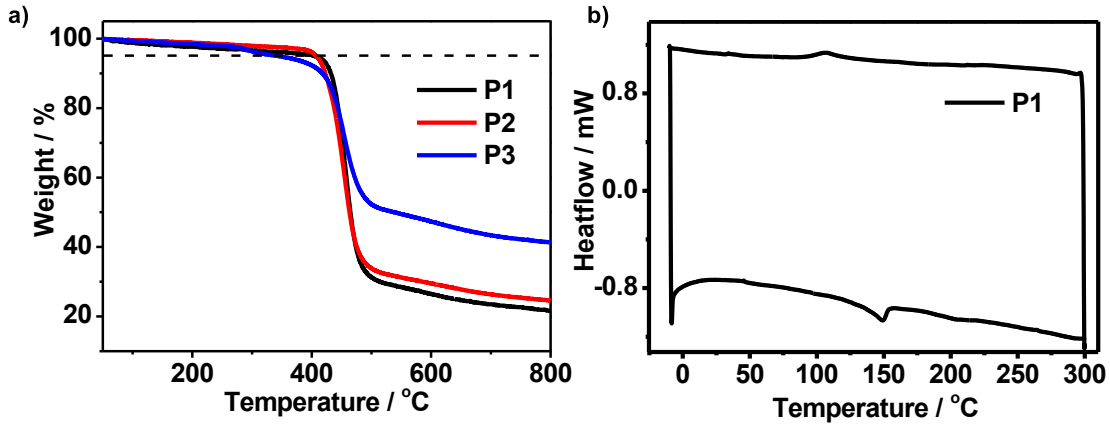

Figure 4. a) TGA curves for polymers **P1**, **P2** and **P3**. b) DSC curve for polymer **P1**.

Cite this: DOI: 10.1039/c0xx00000x

www.rsc.org/xxxxxx

ARTICLE TYPE

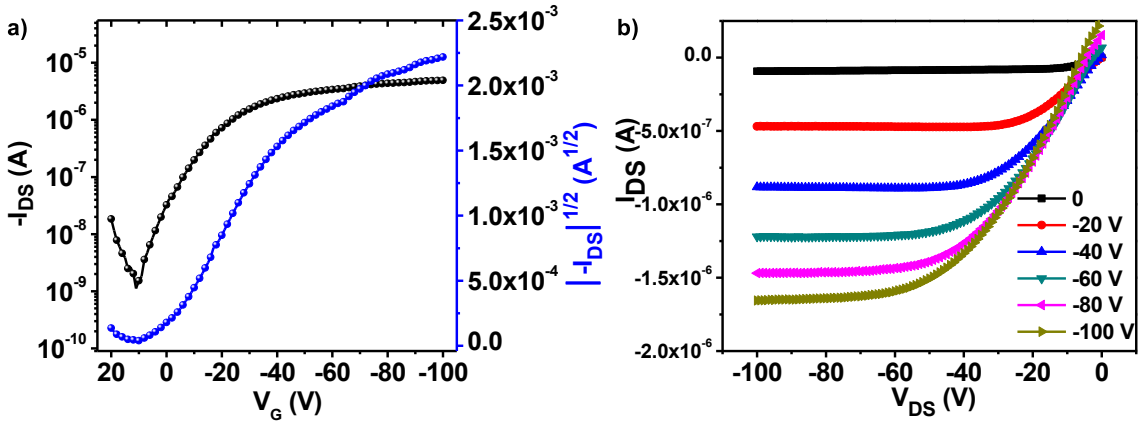

Figure 5. Transfer and output characteristics of OTFT with **P3** thin films (annealed at 160 °C) tested under ambient conditions.

Table 2. Photophysical and electrochemical properties for polymers **P1**, **P2** and **P3**

Polymer	E_{red}^{onset} / V	λ_{abs}^{max} /nm solution	λ_{abs}^{max} /nm film	E_g^{opt} [a] / eV	HOMO [b] / eV	LUMO [b] / eV
P1	-1.03	680	752	1.14	-4.81	-3.67
P2	-0.70	605	720	1.15	-5.15	-4.00
P3	-1.01	770	835	0.93	-4.62	-3.69

[a] the energy gap E_g^{opt} was calculated from the onset edge UV-vis absorption spectra (in film); [b] the HOMO and LUMO energy level were calculated as following equation: LUMO = - (E_{red}^{onset} + 4.80) eV, HOMO = LUMO – E_g^{opt}.[19]

shown in Figure 3, only one quasi-reversible reduction peak was observed for **P1**, with the onset reduction potential (E_{red}^{onset}) at -1.03 V. Polymer **P2** and **P3** exhibited two quasi-reversible reduction peaks with E_{red}^{onset} at -0.70 V and -1.01 V, respectively. No oxidation peaks were observed for all of the three polymers. The LUMO and HOMO energy levels were determined according to the following equations: LUMO = - (E_{red}^{onset} + 4.80) eV, HOMO = LUMO – E_g^{opt}.[19] The LUMO/HOMO energy levels are calculated to be -3.67/-4.81 eV, -4.00/-5.15 eV, and -3.69/-4.62 eV for **P1**, **P2** and **P3**, respectively.

Thermal properties

Thermal stability is one of the key requirements for the practical application of organic electronic materials. The thermal stability of **P1-3** was measured by thermogravimetric analysis (TGA) in N_2 with a heating rate of 10 °C/min. The decomposition temperature (T_d, corresponding to a 5% weight loss) locates at 335, 405, and 406 °C for **P1**, **P2** and **P3**, respectively (Figure 4a), demonstrating their sufficiently high thermal stability for the application of organic electronic materials.

The glass transition temperature of **P1** was observed at 152 °C from the differential scanning calorimetry (DSC) curve (Figure 4b). However, neither obvious glass transition nor other phase transitions were observed below 300 °C for both **P2** and **P3** (Fig. S2 in the ESI†).

Charge transport behaviour

Bottom-gate top-contact OTFTs were fabricated to investigate the charge-transport properties of the NDI-based copolymers **P1**–**P3**. The device performance of **P2** and **P3** is summarized in Table S1 (See transfer and output characteristics in the ESI†, Fig. S3 and Fig. S4). While **P1** shows no TFT signals in the device testing, hole charge-transport characteristics were observed in **P2** and **P3** devices. After thermal annealing at 160 °C, **P2** devices exhibited the hole mobility of only 8 × 10^{-5} cm^2 V^{-1} s^{-1} (on/off = 9 × 10^2, V_{th} = -3.1 V), while **P3** devices revealed an effective

saturation hole mobility of 4.6 × 10^{-3} cm^2 V^{-1} s^{-1} (on/off = 2.18 × 10^3, V_{th} = 11.8 V). For the highest mobility polymer of this series **P3**, we also investigate the device performance as a function of annealing temperatures. Figures S3 and Table S1 (in the ESI†) summarize the device performance characteristics of **P3** after being annealed at different temperatures. At the optimum annealing temperature of 160 ºC (Figure 5), the device exhibited the best performance with hole mobility of 4.6 × 10^{-3} cm^2 V^{-1} s^{-1}. Further increase of annealing temperature led to lower device performance owing to dewetting problem of the polymer on the Si/SiO_2 substrate.

In order to understand the effect of film morphology and phase separation upon thermal annealing on the charge transport in OTFT devices described above, we employed atomic force microscopy (AFM) and X-ray diffraction (XRD) spectrometer to characterize the thin films of **P1**-**3** after being annealed at different temperatures. The results are presented in Supporting Information (Fig. S5-7 in the ESI†). The XRD spectra (Fig. S5 in the ESI†) show that all of the three polymers are amorphous in thin films both at room temperature and after being annealed at a higher temperature (160 ^oC for **P1** and **P2**, and up to 240 ^oC for **P3**), consistent with the DSC results. The AFM results (Fig. S6-7 in the ESI†) indicate that all of the thin films are smooth without obvious phase separation at room temperature. After being annealed at 160 ^oC, the thin film of **P1** showed interesting ordered lamellar phase separation with an average periodic distance of ca. 20 nm. It remains unclear why such ordered phase separation did not lead to high charge carrier transport in TFT devices as described above, which is surprising to us and warrants further investigation. In contrast to **P1**, both P2 and P3 showed phase separation of biocontinuous networks after being thermally annealed, which may contribute to the improvement of charge transport in TFT devices.

We note that only p-channel hole transport was observed in both **P2**- and **P3**-involved TFT devices, which was surprising as ambipolar charge transport was expected given the narrow bandgaps (E_g < 1.1 eV) of both polymers. Recently, Li and coworkers[20] reported a similar phenomenon (i.e. a moderate hole mobility in the order of 10^{-2} cm^2 V^{-1} s^{-1} and no electron transport) in *bottom-gate*, *bottom-contact* OTFT devices in which a poly(2-pyridinyl-DPP-*alt*-bithiophene) (denoted as PDBPyBT) was served as the semiconducting layer. Nevertheless, the same polymer exhibited high ambipolar charge transport behaviour with a record high electron mobility of 6.3 cm^2 V^{-1} s^{-1} and hole mobility of 1~2 cm^2 V^{-1} s^{-1} in *top-gate*, *bottom-contact* OTFT devices. These results imply that further optimization of the OTFT devices, for example, the adoption of top-gate, bottom-contact device configuration and better passivation of the SiO_2/Si surface may lead to higher charge carrier mobility in our polymers (e.g. **P2** and **P3**).

Conclusions

In conclusion, a series of NDI-based alternating narrow-bandgap polymers (**P1**-**3**) have been synthesized through direct arylation polycondensation, with M_n up to 27.4 kDa. The ^1H NMR spectra of these polymers indicate that all polymers correspond to a well-defined alternating copolymer without obvious structural defects such as homocoupling. The polymers show the absorption maximum up to 770 nm in solution and 835 nm in film, with the band gap E_g^{opt} as low as 0.93 eV. All polymers show high thermal stability up to 335 ^oC. With an optimization of annealing temperature at 160 ^oC, **P3** shows a moderate hole mobility of 4.6 × 10^{-3} cm^2 V^{-1} s^{-1} under ambient condition.

We envision that further simplification of the synthetic steps towards these NDI-based narrow-bandgap polymers is possible via exclusive direct arylation coupling that we reported previously.[17b] For example, recent work reported by the Sommer group[21] as well as the Kanbara group[12a] demonstrates that the thiophene-flanked NDI monomers can be synthesized in fewer steps using direct arylation coupling compared to Stille coupling. We believe that the work reported in this article represent a key step further to broadening the scope of high-quality semiconducting polymers that can be synthesized via DAP.

Experimental section

Materials

All reagents were purchased from commercial sources and used without further purification. Anhydrous dichloromethane (DCM), chloroform ($CHCl_3$) and N, N-dimethylformaldehyde (DMF) were distilled from CaH_2. Anhydrous toluene was distilled from sodium/benzophenone immediately prior to use.

General characterization methods

All NMR spectra were recorded on Bruker AMX300 at 300 MHz spectrometers. ^1H NMR and ^{13}C NMR spectra were recorded in CDCl3 at 300 K and in $C_2D_2Cl_4$ at 373 K. All chemical shifts are quoted in ppm, using the residual solvent peak as a reference standard ($CDCl_3$, 7.26 ppm; $C_2D_2Cl_4$, 5.98 ppm). UV-vis absorption spectra were recorded on Shimadzu UV-2450 and Varian UV-vis-NIR spectrometers in analytical grade solvents. Cyclic voltammetry was performed on a CHI 620C electrochemical analyzer with a three-electrode cell in a solution of 0.1M tetrabutylammonium hexafluorophosphate (Bu_4NPF_6) dissolved in dry DCM at a scan rate of 50 mV s^{-1}. A Pt electrode with a diameter of 2 mm, a Pt wire and an Ag/AgCl electrode were used as the working electrode, the counter electrode and the reference electrode, respectively. The potential was calibrated against the ferrocene/ferrocenium couple. Thermogravimetric analysis (TGA) was carried out on a TA instrument 2960 at a heating rate of 10 ºC/min under N_2 flow, differential scanning calorimetry (DSC) was performed on a TA instrument 2920 at a heating/cooling rate of 10 ºC/min under N_2 flow. The XRD patterns were obtained by Bruker 6000 X-ray diffractometer using a Cu K α source. AFM images were obtained by using Dimension 3100 (Veeco, CA) in tapping mode with a Si tip (Veeco, resonant frequency, 320 kHz; spring constant, 42 N/m) under ambient conditions with a scanning rate of 1 Hz and scanning line of 512.

Transistors were fabricated in the bottom-gate/top-contact configuration on highly doped n-type Si substrates with 300-nm-thick thermally grown silicon dioxide as the dielectric layer. The Si substrates were successively ultra-sonicated in detergent, water, acetone and iso-propyl alcohol. Octyldecyltrichlorosilane

(OTS, purchased from Aldrich) monolayer was deposited by placing the substrates in 0.1% (v/v) toluene solution overnight under nitrogen, ultrasonicated in toluene for 15 mins and dried at 140 ºC. The capacitance per unit area of the gate dielectric layer (SiO_2, 300 nm) was C_i = 11.5 nF cm^{-2}. The solutions were filtered through poly(tetrafluoroethylene) (PTFE, 0.2 μm) filters prior to film deposition. All the organic thin films were spuncast onto the OTS layer from chloroform solutions (10 mg mL^{-1}) at a rotation rate of 2000 rpm for 60 s. Finally, gold source/drain electrodes (80 nm thick) were evaporated on top through a metal mask (12 pixels/chip) with various channel lengths (L = 100-225 μm) and width (W = 4 or 2 mm) dimensions. The thermal deposition was performed on the hotplate in glovebox filled with N2. Sample annealing was carried out for 30 mins to 1 h, and followed by slow cooling to room temperature in 1 h. The OTFT devices were then characterized using a Keithley SCS-4200 semiconductor parameter analyser under ambient condition. For each condition, 8-12 devices were tested. The field-effect mobility was calculated from the following equation in the saturation regime: $I_{ds} = (W/2L)C_i\mu(V_{gs}-V_{th})^2$, where W and L are the channel width and length, respectively. C_i is the capacitance of the insulating SiO_2 layer per unit, V_{gs} and V_{th} are the gate voltage and the threshold voltage, respectively.

Synthesis

4,9-dibromo-2,7-bis(2-octyldodecyl)benzo[lmn][3,8]phenanth -roline -1,3,6,8(2H,7H)-tetraone (**2**).

A suspension of 4,9-dibromoisochromeno[6,5,4-*def*]isochromene-1,3,6,8-tetraone **1** (0.426 g, 1 mmol), 2-decyltetradecan-1-amine (1.190 g, 4 mmol) and HOAc (10 mL). The mixture was heated to 135 °C for 30 min under Ar (g). After cooling to room temperature, the mixture was extracted with $CHCl_3$ (50 mL × 2). The combined organic phase was washed with brine (100 mL × 3) and saturated $NaHCO_3$ (100 mL × 1), then dried over anhydrous Na_2SO_4. The organic solvent was removed under reduced pressure and the residue was purified by column chromatography (silica gel, EA:Hex = 1:10) to afford compound **3** as pink solid (0.246 g, 25%). ^{1}H NMR (300 MHz, $CDCl_3$, 300 K): δ ppm = 8.98 (s, 2H), 4.14 (d, *J* = 7.5 Hz, 2H), 1.98 (br, 2H), 1.30-1.23 (m, 64H), 0.87-0.83 (m, 1H)

4,9-bis(4-(2-ethylhexyl)thiophen-2-yl)-2,7-bis(2-octyldodecyl)benzo[*lmn*][3,8]phenanthroline-1,3,6,8(2H,7H)-tetraone (**4**).

A mixture of compound **2** (0.985 g, 1 mmol), (4-(2-ethylhexyl)thiophen-2-yl) trimethylstannane (0.900 g, 2.5 mmol) and catalyst $PdCl_2(PPh_3)_2$ (70 mg, 0.1 mmol) in anhydrous DMF (3 mL) and toluene (30 mL) was degassed by three freeze–pump–thaw cycles. The mixture was heated to 110 °C under argon for overnight. The mixture was cooled to room temperature and extracted with $CHCl_3$ (100 mL × 2). The combined organic phase was washed with $NaHCO_3$ (100 mL× 2) and brine (100 mL × 1). The organic phase was dried over anhydrous Na_2SO_4, and the organic solvent was removed under reduced pressure. The crude product was purified by column chromatography (silica gel, $CHCl_3$/Hex = 1:10) to afford compound **4** as purple wax solid (1.115 g, 92%). ^{1}H NMR (300 MHz, $CDCl_3$, 300 K): δ ppm = 8.75 (s, 2H), 7.12-7.11 (m, 4H), 4.07 (d, *J* = 7.5 Hz, 4H), 2.63 (d, *J* = 6.9 Hz, 4H), 1.95 (m, 2H), 1.63-1.61 (m, 2H), 1.33-1.22 (m, 80H), 0.95-0.82 (m, 24H); ^{13}C NMR (75 MHz, $CDCl_3$, 300 K): δ ppm = 162.62, 162.34, 142.38, 140.36, 140.16, 136.49, 130.28, 127.32, 125.21, 123.77, 122.96, 44.85, 40.34, 36.46, 34.57, 32.51, 31.86, 31.61, 30.01, 29.59, 29.52, 29.30, 29.26, 28.92, 26.43, 25.57, 23.03, 22.63, 22.62, 14.13, 14.06, 10.82.

4,9-bis(5-bromo-4-(2-ethylhexyl)thiophen-2-yl)-2,7-bis(2-octyldodecyl)benzo[*lmn*][3,8]phenanthroline-1,3,6,8(2H,7H)-tetraone (**5**).

To a 100 mL of round bottom flask equipped with a magnetic stirring bar, **4** (1.115 g, 0.92 mmol) was dissolved in a mixture of $CHCl_3$ (20 mL) and DMF (20 mL). The resulting solution was cooled in an ice bath and NBS (0.495 g, 2.76 mmol) was added in one portion. Stirring was continued in the ice bath for overnight and the mixture was poured into water. The mixture was extracted twice with DCM (100 mL x 2) and the combined organic layer was dried over anhydrous magnesium sulphate. Concentration of the solvent under reduced pressure left a crude oil, which was purified by column chromatography (silica gel, EA/Hex = 1:20) on to afford **5** as purple wax solid (1.200 g, 95%). ^{1}H NMR (300 MHz, $CDCl_3$, 300 K): δ ppm = 8.71 (s, 2H), 7.01 (s, 2H), 4.08 (d, *J* = 7.2 Hz, 4H), 2.58 (d, *J* = 8.1 Hz, 4H), 1.95 (m, 2H), 1.69 (m, 2H), 1.42-1.23 (m, 80H), 0.97-0.82 (m, 24H) ^{13}C NMR (75 MHz, $CDCl_3$, 300 K): δ ppm = 162.42, 162.29, 141.69, 139.90, 139.34, 136.26, 130.21, 127.43, 125.43, 122.83, 113.09, 44.95, 39.94, 36.49, 33.87, 32.51, 31.88, 31.61, 30.04, 29.62, 29.55, 29.32, 29.29, 28.82, 26.40, 25.63, 23.06, 22.66, 22.65, 14.14, 14.09, 10.79.

4,6-di-(2-thienyl)thieno[3,4-*c*][1,2,5]thiadiazole (**7**, **TTD**)

To a 100 mL of round bottom flask equipped with a magnetic stirring bar, **6** (0.825 g, 2.5 mmol) was added into a mixture of THF (30 mL), MeOH (15 mL) and HCl (37%, 15 mL), N_2 (g) was purged into the mixture for 10 min, then $SnCl_2.2H_2O$ (6.769 g, 30 mmol, 12 eq) was added in one portion, later the mixture was kept stirring overnight at 50 °C. After cooling to room temperature, the mixture was quenched with NaOH (10%, aq), and extracted with ethyl acetate (200 mL × 2). The combined organic phase was washed with NaOH (10%, aq) (100 mL × 3). The organic phase was dried over anhydrous Na_2SO_4, and the organic solvent was removed under reduced pressure. The crude product was achieved as dark liquid. After drying for 3 h, PhNSO (0.672 mL), TMSCl (2.23 mL), anhydrous Et_3N (30 mL) and anhydrous $CHCl_3$ (30 mL) was added slowly. The reaction mixture was heated to 50 °C for overnight. The mixture was cooled to room temperature and extracted with ethyl acetate (100 mL × 2). The combined organic phase was washed with HCl (10%, aq, 200 mL× 2) and brine (200 mL × 1). The organic phase was dried over anhydrous Na_2SO_4, and the organic solvent was removed under reduced pressure. The crude product was purified by column chromatography (silica gel, $CHCl_3$/Hex = 1:20) to afford **TTD 7** as purple blue solid (580 mg, 76%, based on 6). ^{1}H NMR (300 MHz, CDCl3, 300 K): δ ppm = 7.54 (dd, J_1= 0.9 Hz, J_2 = 3.75 Hz, 2H), 7.31 (dd, J_1 = 0.9 Hz, J_2 = 5.1 Hz, 2H), 7.09 (dd, J_1 = 0.9 Hz, J_2 = 5.1 Hz, 2H)

Copolymer P1.

In a glove box, **5** (182 mg, 0.15 mmol), **EDOT** (**8**) (21 mg, 0.15 mmol), $Pd_2(dba)_3$ (7 mg, 5% mmol), (o-MeOPh)$_3$P (6 mg, 10% mmol), K_2CO_3(104 mg, 0.75 mmol, 5 eq) , PivOH (8 mg, 0.5 eq) and solvent *o*-xylene (1.5 mL) were added in a microwave reaction vial with a magnetic stirring bar. The vial was sealed with a cap and then removed from the glove box. The vial was heated in a 100 ^oC oil bath for 24 hours. After being cooled to room temperature, the reaction mixture was diluted with 30 mL of chloroform and then filtered to remove the insoluble species. The filtrate was concentrated and added dropwise to 100 mL of methanol, filtered through a Soxhlet thimble, and then subjected to Soxhlet extraction with methanol, acetone and n-Hexane sequentially. The n-Hexane fraction was concentrated and precipitated in 100 mL of methanol. The precipitates were collected by filtration to achieve the target polymer as a green solid (158 mg, 77%). GPC (THF at 23 ^oC): M_n = 16.4 kg mol^{-1}, M_w = 33.3 kg mol^{-1}, and PDI = 2.0 (against PS standard). ^{1}H NMR (300 MHz, $C_2D_2Cl_4$, 373 K): δ ppm = 8.86 (s, 2H), 7.28 (s, 2H), 4.44 (s, 4H), 4.16 (br, 4H), 2.89 (br, 4H), 2.08 (br, 2H), 1.82 (br, 2H), 1.48- 1.28 (m, 112H), 0.98- 0.89 (m, 30H).

Copolymer P2.

In a glove box, **5** (182 mg, 0.15 mmol), **9 DPP** (78 mg, 0.15 mmol), $Pd_2(dba)_3$ (7 mg, 5% mmol), (o-MeOPh)$_3$P (6 mg, 10% mmol), K_2CO_3 (104 mg, 0.75 mmol, 5 eq) , PivOH (8 mg, 0.5 eq) and solvent *o*-xylene (1.5 mL) were added in a microwave reaction vial with a magnetic stirring bar. The vial was sealed with a cap and then removed from the glove box. The vial was heated in a 100 ^oC oil bath for 24 hours. After being cooled to room temperature, the reaction mixture was diluted with 30 mL of chloroform and then filtered to remove the insoluble species. The filtrate was concentrated and added dropwise to 100 mL of methanol, filtered through a Soxhlet thimble, and then subjected to Soxhlet extraction with methanol, acetone and n-Hexane sequentially. The n-hexane fraction was concentrated and precipitated in 100 mL of methanol. The precipitates were collected by filtration to achieve the target polymer as a green solid (200 mg, 79%). GPC (THF at 23 ^oC): M_n = 27.4 kg mol^{-1}, M_w = 50.5 kg mol^{-1}, and PDI = 3.0 (against PS standard). ^{1}H NMR (300 MHz, $C_2D_2Cl_4$, 373 K): δ ppm = 8.98 (br, 2H), 8.85 (s, 2H), 7.44 (br, 2H), 7.69 (br, 2H), 7.28 (s, 2H), 4.14 (br, 8H), 2.92 (br, 4H), 2.05 (br, 2H), 1.86 (br, 2H), 1.47- 1.28 (m, 120H), 1.00- 0.88 (m, 40H).

Copolymer P3.

In a glove box, **5** (182 mg, 0.15 mmol), **7 TTD** (46 mg, 0.15 mmol), $Pd_2(dba)_3$ (7 mg, 5% mmol), (o-MeOPh)$_3$P (6 mg, 10% mmol), K_2CO_3(104 mg, 0.75 mmol, 5 eq) , PivOH (8 mg, 0.5 eq) and solvent *o*-xylene (1.5 mL) were added in a microwave reaction vial with a magnetic stirring bar. The vial was sealed with a cap and then removed from the glove box. The vial was heated in a 100 ^oC oil bath for 24 hours. After being cooled to room temperature, the reaction mixture was diluted with 30 mL of chloroform and then filtered to remove the insoluble species. The filtrate was concentrated and added dropwise to 100 mL of methanol, filtered through a Soxhlet thimble, and then subjected to Soxhlet extraction with methanol, acetone, ethyl acetate and chloroform sequentially. The chloroform fraction was concentrated and precipitated in 100 mL of methanol. The precipitates were collected by filtration to achieve the target polymer as a green solid (193 mg, 85%). GPC (THF at 23 ^oC): M_n = 17.0 kg mol^{-1}, M_w = 55.4 kg mol^{-1}, and PDI = 3.2 (against PS standard). ^{1}H NMR (300 MHz, $C_2D_2Cl_4$, 373 K): δ ppm = 8.86 (s, 2H), 7.69 (br, 2H), 7.31-7.29 (m, 4H), 4.16 (br, 4H), 2.92 (br, 4H), 2.07(br, 2H), 1.86 (br, 2H), 1.47- 1.28 (m, 115H), 1.00- 0.89 (m, 30H).

Acknowledgements

M.W. thanks the funding support by a start-up grant from Nanyang Technological University, and AcRF Tier 1 (M4011061.120, RG49/12) from the Ministry of Education, Singapore. We thank Prof. Yuan Chen for access to the UV-VIS-NIR spectrometer.

Notes and references

School of Chemical and Biomedical Engineering, Nanyang Technological University, 62 Nanyang Drive, Singapore 637459, Singapore. E-mail: mfwang@ntu.edu.sg; Fax: +65 6794 7553; Tel: +65 6316 8746
†Electronic Supplementary Information (ESI) available: See DOI: 10.1039/b000000x/

1. a) A. C. Grimsdale, K. L. Chan, R. E. Martin, P. G. Jokisz and A. B. Holmes, *Chem. Rev*. 2009, 109, 897. b) F. Huang, H. B. Wu and Y. Cao, *Chem. Soc. Rev*. 2010, 39, 2500.
2. a) C. L. Wang, H. L. Dong, W. P. Hu, Y. Q. Liu and D. B. Zhu, *Chem. Rev*. 2012, 112, 2208. b) Y. F. Deng, Y. G. Chen, X. J. Zhang, H. K. Tian, C. Bao, D. H. Yan, Y. H. Geng and F. S. Wang, *Macromolecules* 2012, 45, 8621. c) J. G. Mei, Y. Diao, A. L. Appleton, L. Fang and Z. N. Bao, *J. Am. Chem. Soc*. 2013, 135, 6724. d) A. Facchetti, *Nat. Mater*. 2013, 12, 598–599. e) H. N. Tsao and K. M€ullen, *Chem. Soc. Rev*. 2010, 39, 2372. f) Y. Takeda, T. L. Andrew, J. M. Lobez, A. J. Mork and T. M. Swager, *Angew. Chem. Int. Ed*. 2012, 51, 9042.
3. a) L. J. A. Koster, S. E. Shaheen and J. C. Hummelen, *Adv. Energy Mater*. 2012, 2, 1246. b) J. L. Li, A. C. Grimsdale, *Chem. Soc. Rev*. 2010, 39, 2399. c) H.-Y. Chen, J. H. Hou, S. Q. Zhang, Y. Y. Liang, G. W. Yang, Y. Yang, L. P. Yu, Y. Wu and G. Li, *Nat. Photonics* 2009, 3, 649. d) L. J. Huo, S. Q. Zhang, X. Guo, F. Xu, Y. F. Li and J. H. Hou, *Angew. Chem. Int. Ed*. 2011, 50, 9697. e) Z. C. He, C. M. Zhong, S. J. Su, M. Xu, H. B. Wu and Y. Cao, *Nat. Photonics* 2012, 6, 591. f) J. B. You, L. T. Dou, K. Yoshimura, T. Kato, K. Ohya, T. Moriarty, K. Emery, C. Chen, J. Gao, G. Li and Y. Yang, *Nat. Commun*. 2013, 4, 1446.
4. a) B. Carsten, F. He, H. J. Son, T. Xu and L. P. Yu, *Chem. Rev*. 2011, 111, 1493b) K. Okamoto, C. K. Luscombe, *Polym. Chem*. 2011, 2, 2424. c) J. Sakamoto, M. Rehahn, G. Wegner and A. D. Schl€uter, *Macromol. Rapid Commun*. 2009, 30, 653. d) C. Amatore, A. Jut and, G. Le Duc, *Angew. Chem. Int. Ed*. 2012, 51, 1379.
5. For a recent review, see a) P. P. Khlyabich, B. Burkhart, A. E. Rudenko and B. C. Thompson, *Polymer,* 2013, 54, 5267. b) K. Okamoto, J. X. Zhang, J. B. Housekeeper, S. R. Marder and C. K. Luscombe, *Macromolecules*, 2013, 46, 8059. c) L. G. Mercier and M. Leclerc, *Acc. Chem. Res*., 2013, 46, 1597. d) K. Wang and M. F. Wang, *Curr. Org. Chem*., 2013, 17, 999. e) A. E. Rudenko and B. C. Thompson, *J. Polym. Sci., Part A: Polym. Chem*. 2015, 53, 135.
6. a)S. V. Bhosale, S. V. Bhosale and S. K. Bhargava, *Org. Biomol. Chem*. 2012, 10, 6455. b) F. S. Kim, X. Guo, M. D. Watson and S. A. Jenekhe, *Adv. Mater*. 2010, 22, 478. c) M. M. Durban, P. D. Kazarinoff and C. K. Luscombe, *Macromolecules* 2010, 43, 6348. d) X. Guo, F. S. Kim, M. J. Seger, S. A. Jenekhe and M. D. Watson, *Chem. Mater*. 2012, 24, 1434. e) R. Steyrleuthner, M. Schubert, I. Howard, B. Klaumunzer, K. Schilling, Z. Chen, P. Saalfrank, F. Laquai, A. Facchetti and D. Neher, *J. Am. Chem. Soc*. 2012, 134, 18303. f) E. Zhou, J. Cong, M. Zhao, L. Zhang, K. Hashimoto and K. Tajima, *Chem. Commun*. 2012, 48, 5283.

7. a) K. Nakabayashi and H. Mori, *Macromolecules* 2012, 45, 9618. b) Y.-J. Hwang, G. Ren, N. M. Murari and S. A. Jenekhe, *Macromolecules* 2012, 45, 9056. c) M. Yuan, M. M. Durban, P. D. Kazarinoff, D. F. Zeigler, A. H. Rice, Y. Segawa and C. K. Luscombe, *J. Polym. Sci., Part A: Polym. Chem*. 2013, 51, 4061.
8. S.-W. Chang, H. Waters, J. Kettle, Z.-R. Kuo, C.-H. Li, C.-Y. Yu and M. Horie, *Macromol. Rapid Commun*. 2012, 33, 1927.
9. K. Nakabayashi and H. Mori, *Chem. Lett*. 2013, 42, 717.
10. A. Luzio, D. Fazzi, F. Nubling, R. Matsidik, A. Straub, H. Komber, E. Giussani, S. E. Watkins, M. Barbatti, W. Thiel, E. H Gann, L. Thomsen, C. R. McNeill, M. Caironi and M. Sommer, *Chem. Mater.* 2014, 26, 6233.
11. X. Guo, A. Facchetti, and T. J. Marks, *Chem. Rev*. 2014, 114, 8943.
12. a) Y. Nohara, J. Kuwabara, T. Yasuda, L. Han and T. Kanbara, *J. Polym. Sci. Part A: Polym. Chem*. 2014, 52, 1401. b) R. Matsidik, H. Komber, A. Luzio, M. Caironi, and M. Sommer, *J. Am. Chem. Soc.*, 2015, *137*, 6705.
13. X. Guo and M. D. Watson, *Org. Lett*. 2008, 10, 5333.
14. S. Steinberger , A. Mishra , E. Reinold , E. Mena-Osteritz , H. Müller , C. Uhrich , M. Pfeiffer and P. Bäuerle , *J. Mater. Chem*. 2012, 22, 2701.
15. a) P. Karsten, J. C. Bijleveld, L. Viani, J. Cornil, J. Gierschner and R. A. J. Janssen, *J. Mater. Chem*., 2009, 19 , 5343. b) Y. J. Hwang, F. S. Kim, H. Xin and S. A. Jenekhe, *Macromolecules*, 2012, 45, 3732.
16. L. Ying, B. B. Y. Hsu, H. Zhan, G. C. Welch, P. Zalar, L. A. Perez, E. J. Kramer, T.-Q. Nguyen, A. J. Heeger, W.-Y. Wong and G. C. Bazan, *J. Am. Chem. Soc*. 2011, 133, 18538.
17. a) X. Wang and M. Wang, *Polym. Chem.*, 2014, 5, 5784. b) X.. Wang, K. Wang and M. Wang, *Polym. Chem.*, 2015, 6, 1846.
18. a) P. Berrouard, A. Najari, A. Pron, D. Gendron, P.-O. Morin, J.-R. Pouliot, J. Veilleux and M. Leclerc, *Angew. Chem., Int. Ed*. 2012, 51, 2068–2071. b) X. Zhang, Y. Gao, S. Li, Xi. Shi, Y. Geng and F. Wang, *J. Polym. Sci. A Polym. Chem*. 2014, 52, 2367.
19. a) A. J. Bard, L. R. Faulkner, Electrochemical Methods: Fundamentals and Applications, Wiley, New York, 1984. b) J. Pommerehne, H. Vestweber, W. Guss, R. F. Mahrt, H. Bassler, M. Porsch and J. Daub, *Adv. Mater*. 1995, 7, 551. c) J. Shao, J. Chang and C. Chi. *Chem- An Asian Journal,* 2014, 9, 253. d) J. Shao, J. Chang, G. Dai and C. Chi. *J. Polym. Sci. A Polym. Chem*. 2014, 52, 2454. e) J. Shao, J. Chang and C. Chi. *Org. Biomol. Chem.,* 2012, 10, 7045.
20. B. Sun, W. Hong, Z. Yan, H. Aziz, Y. Li, *Adv. Mater*. 2014, 26, 2636.
21. R. Matsidik, J. Martin, S. Schmidt, J. Obermayer, F. Lombeck, F. Nübling, H. Komber, D. Fazzi, and M. Sommer *J. Org. Chem.*, 2015, *80*, 980.

Direct Arylation Polycondensation for Efficient Synthesis of Narrow-Bandgap Alternating D-A Copolymers Consisting of Naphthalene Diimide as Acceptor

Jinjun Shao, Guojie Wang, Kai Wang, Cangjie Yang, Mingfeng Wang*

TOC Figure

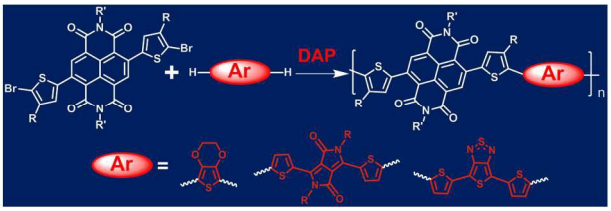

Direct arylation polycondensation enables efficient synthesis of narrow-bandgap, well-defined alternating D-A copolymers consisting of naphthalene diimide as the acceptor unit.